Journal of Plant Physiology xxx (xxxx) xxx–xxx

Contents lists available at ScienceDirect

Journal of Plant Physiology

journal homepage: www.elsevier.com/locate/jplph

Hydraulic conductivity of soil-grown lupine and maize unbranched roots and maize root-shoot junctions

Félicien Meunier[a], Mohsen Zarebanadkouki[b,*], Mutez A. Ahmed[b,d,e], Andrea Carminati[b], Valentin Couvreur[f], Mathieu Javaux[a,c]

[a] Earth and Life Institute, Environmental sciences, Université catholique de Louvain, B-1348 Louvain-la-Neuve, Belgium
[b] Division of Soil Physics, University of Bayreuth, Bayreuth, Germany
[c] Institute of Bio- and Geosciences, IBG-3 Agrosphere, Forschungszentrum Jülich GmbH, D-52425 Jülich, Germany
[d] Division of Soil Hydrology, University of Goettingen, D-37077 Göttingen, Germany
[e] Department of Agricultural Engineering, Faculty of Agriculture, University of Khartoum, Khartoum, Sudan
[f] Earth and Life Institute, Agronomic sciences, Université catholique de Louvain, B-1348 Louvain-la-Neuve, Belgium

ARTICLE INFO

Keywords:
Maize root types
Root hydraulic conductance
Root pressure probe
Radial conductivity
Axial conductivity
Lupine lateral roots
Root-shoot junction

ABSTRACT

Improving or maintaining crop productivity under conditions of long term change of soil water availability and atmosphere demand for water is one the big challenges of this century. It requires a deep understanding of crop water acquisition properties, i.e. root system architecture and root hydraulic properties among other characteristics of the soil-plant-atmosphere continuum. A root pressure probe technique was used to measure the root hydraulic conductances of seven-week old maize and lupine plants grown in sandy soil. Unbranched root segments were excised in lateral, seminal, crown and brace roots of maize, and in lateral roots of lupine. Their total hydraulic conductance was quantified under steady-state hydrostatic gradient for progressively shorter segments. Furthermore, the axial conductance of proximal root regions removed at each step of root shortening was measured as well. Analytical solutions of the water flow equations in unbranched roots developed recently and relating root total conductance profiles to axial and radial conductivities were used to retrieve the root radial hydraulic conductivity profile along each root type, and quantify its uncertainty. Interestingly, the optimized root radial conductivities and measured axial conductances displayed significant differences across root types and species. However, the measured root total conductances did not differ significantly. As compared to measurements reported in the literature, our axial and radial conductivities concentrate in the lower range of herbaceous species hydraulic properties. In a final experiment, the hydraulic conductances of root junctions to maize stem were observed to highly depend on root type. Surprisingly maize brace root junctions were an order of magnitude more conductive than the other crown and seminal roots, suggesting potential regulation mechanism for root water uptake location and a potential role of the maize brace roots for water uptake more important than reported in the literature.

1. Introduction

Global crop production is negatively affected by drought, which is the most significant abiotic stress in agriculture (Cattivelli et al., 2008). This stress can be defined as the plant's inability to take up and transport water to the shoot at the rate required to sustain transpiration, with such inability leading to stomata closure and reduced yield (Farooq et al., 2009). The extraction of water from soil and supply to the shoot to maintain the transpiration and the carbon capture for photosynthesis is one of the major roles of the root systems (McElrone et al., 2013). Recently, it has received increasing attention as a promising target for breeding drought-tolerant crops in a climate change context (Comas et al., 2013; Hammer et al., 2009; Schoppach et al., 2014).

Both architectural and hydraulic properties of the root system determine the location and uptake rate of water (Leitner et al., 2014), and by extension its availability (Couvreur et al., 2014). These properties are captured in the concept of “hydraulic architecture” that facilitates the water uptake that is driven by the transpiration demand of the atmosphere (Doussan et al., 1998a; Lobet et al., 2014). From the

Abbreviations: L, length; T, time; P, pressure

* Corresponding author.
E-mail address: mohsen.zarebanadkouki@uni-bayreuth.de (M. Zarebanadkouki).

https://doi.org/10.1016/j.jplph.2017.12.019
Received 24 August 2017; Received in revised form 19 December 2017; Accepted 20 December 2017

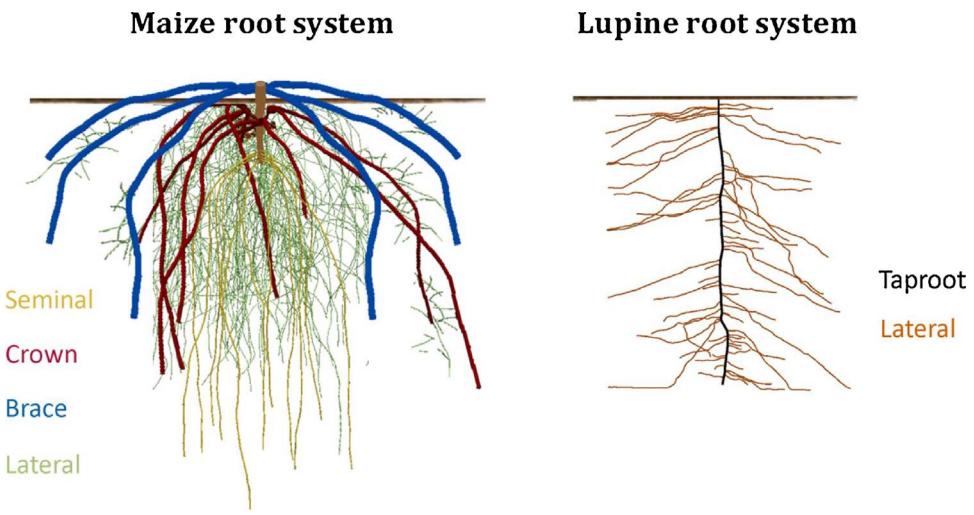

Fig. 1. Schematics of maize (left) and lupine (right) root systems, respectively simulated in CRootBox and observed in rhizotron. Root nomenclature and color code are consistent throughout the manuscript.

hydraulic perspective, the flow of water between soil-root interfaces and xylem vessels is regulated by root radial hydraulic conductivity, which depends on anatomical and physiological properties of the root cross-section (Steudle, 2000). Beyond that point, water transfer up to the shoot is controlled by root axial conductance (Passioura, 1980), which depends on the size, the abundance and the maturation level of the xylem vessels (Martre et al., 2000; Sanderson et al., 1988).

From the architectural perspective, root types and branching patterns impact soil exploration and resource capture in a dynamic way, with strategic consequences on plant fitness to its environment (Draye et al., 2010; Lynch, 2013; Lynch and Brown, 2012). In plants with adventitious root systems, such as maize, the root system consists of four different root types classified as primary, seminal, crown, and brace root (see left panel in Fig. 1, simulated in the software CRootBox (Schnepf et al., 2017)). From these main root axes, the substantial amount of lateral roots that branches out would play a critical role in water acquisition (Ahmed et al., 2016). Lupine (*Lupins Albus* L.), on the contrary, only develops a single primary "tap" root, which branches into laterals of different orders (see right panel in Fig. 1, observed in rhizotron (Zarebanadkouki et al., 2016)). How these root orders translate into different root segment hydraulic properties is still not clear from the literature (Vadez, 2014). In addition, as a result of different growth and maturation rates, these different types of roots will also have a different evolution of their radial and axial hydraulic properties along the axis as a function of their age (Vetterlein and Doussan, 2016). The resulting combination of architecture and root property distribution (called hydraulic architecture) will define the root system conductance.

Although root hydraulic properties partially control water uptake pattern in heterogeneous environments (Javaux et al., 2008; Zarebanadkouki et al., 2016) and have an important breeding potential (Schoppach et al., 2014; Vadez, 2014), their measurement remains challenging, in particular for plants growing in soil. Yet, their accurate determination would allow breeders to better understand how root hydraulics combines to architectural traits, in the determination of species and/or genotypes performances in water-limited environments (Meunier et al., 2017; Meunier et al., 2016b; Tardieu, 2012; Tardieu et al., 2015).

The objective of this study is to evaluate the variability of hydraulic properties along different root types in maize and lateral roots in lupine, as well as the conductance of junctions between the shoot and the principal roots in maize (i.e. the particular zones connecting maize main roots and the stem in the way of the sapflow towards the leaves). This will improve the understanding of the contribution of specific root types and root regions to the overall root conductivity, and their consequences on water uptake patterns.

To do so, we develop methods to characterize root hydraulic properties for different root types. A root pressure probe technique is used to measure profiles of axial and total hydraulic conductances along roots of maize and lupine plants grown in soil, as well as the conductance of root-stem junctions in maize. These measurements are combined with an inverse modeling scheme to retrieve the profile of radial hydraulic conductivity of each root type. These values are finally compared with direct and inverse measurements reported in the literature.

2. Materials and methods

2.1. Soil and plant material

Nine maize and nine lupine plants were grown in aluminium containers (size of 40 × 40 × 1 cm) filled with sandy soil (92% sand – 5% silt – 3% clay). The aluminium containers consisted in two aluminium plates of 40 × 40 cm, which were held together at the edges by aluminium bars of 1 × 1 × 1 cm. This construction enabled us to open the container from one side and carefully dig out roots from soil. Maize seeds were soaked in 10% H_2O_2 solution for 10 min and then germinated on moist filter paper for 48 h. One seedling was then planted at a depth of 1 cm into each container and the upper soil layers were covered with a 1 cm layer of quartz gravel to reduce evaporation from soil surface. The plants were grown with a daily light cycle of 14 h and 10 h of darkness, a light intensity of 500 $\mu mol\, m^{-2}\, s^{-1}$, day and night temperature of 24 and 19 °C, respectively and relative humidity of 60%. During the growth period, plants were irrigated every four days to keep soil at an average water content of 0.20–0.25 $cm^3\, cm^{-3}$. When plants were seven-week old, the containers were opened from one side and roots were carefully washed from the soil. Unbranched segments of different root types of maize (lateral, seminal, crown, and brace roots) and lateral roots of lupine were excised and connected to a pressure probe to measure their hydraulic properties (Bramley et al., 2009; Frensch and Steudle, 1989). The methodology was applied to the different species and root types. For lupine, we only considered the lateral roots since the taproot is rapidly branched. For maize, we analysed seminal, crown, brace and lateral unbranched roots as well as the conductance of the root-shoot junction. Four to five replicates per root type were considered. The procedure of root pressure probe experiment was slow. Three to four root segments per day could be characterized. To avoid age variation among the sampled roots, the nine plants were

grown at three days intervals.

2.2. Root pressure probe

A root pressure probe consists in a pressure transducer located within a capillary connected to the basal end of an excised root; see probe details in Steudle and Boyer (1985). The connection was sealed with silicone material (Xantopren L blue, Heraeus Kulzer GmbH, Germany), which ensured a tight connection without blocking the xylem vessels. The pressure probe was positioned horizontally and the root supported by a glass container (10 × 30 cm) filled with water. Half of the capillary (diameter of 600 µm) was filled with silicon oil and the other half of the capillary facing the root was filled with water. The movement of the meniscus between water and oil was controlled by a metal rod, used to measure the water volume injected into or sucked from the base of the root.

2.3. Root total conductance

Unbranched roots 5–40 cm long were successively connected to the root pressure probe. When the root pressure reached a stable equilibrium value (Ψ_0) (it took around 30–120 min for the different root types), a series of pressure clamps was carried out (3–5 clamps) to induce water flow across the root. The applied pressure was increased in 0.02–0.05 MPa increments (Ψ_1, Ψ_2, …) and held constant at each increment for 10–120 s by continually adjusting the metal rod inside the pressure chamber of the probe (see left panel in Fig. 2). Only the cut end of the root was exposed to the pressure application.

The distance that the metal rod had moved was used to calculate the cumulative water volume, and retrieve the average water flow rates across the root (J_{x1}, J_{x2}, …) [$L^3\,T^{-1}$]. The slope of the linear regression of flow rates plotted against the applied pressure differences yields the root total conductance "K_{root}" [$L^3P^{-1}T^{-1}$] (i.e. conductance that includes both axial and radial components) for the current root length "l" [L] (see right panel in Fig. 2):

$$K_{root} = \frac{J_x}{\Delta\Psi} \tag{1}$$

where $\Delta\Psi$ is the difference between the applied and equilibrated pressure. For details, see Appendix A and Meunier et al. (2017).

As illustrated in Fig. 3(a), after proceeding to the measurement of K_{root} with root length l_1, a small proximal root segment (2 cm) was cut off with a razor blade, and the root was reconnected to the pressure probe to carry out the measurement of K_{root} for root length l_2. This cycle was repeated until the root tip.

2.4. Root axial conductance

The root intrinsic axial hydraulic conductance (k_x) [$L^4P^{-1}T^{-1}$] is a local root property defined as the product of the length of a root segment (l_{seg}) [L] by its axial hydraulic conductance. Each time a 2-cm root segment was cut off from the root proximal end, its axial conductance was measured with a series of pressure clamps after the new equilibrium pressure was attained (see left panel of Fig. 2, and scheme of the small root segment in Fig. 3a). The calculation process was similar to that of K_{root}, and the following equation applied (see Appendix A for details):

$$k_x = \frac{J_x l_{seg}}{\Delta\Psi} \tag{2}$$

Note that the measured axial conductance was assigned to the middle position of the root segment along the axis of distances to the tip "z"; see for instance z_1 in Fig. 3(a), in order to obtain a profile of k_x as a function of z. Again only the cut end of the root segment was exposed to the pressure application.

2.5. Junctions to shoot conductance

A simple version of the high pressure flowmeter method was used to determine the axial hydraulic conductance of root-shoot junction (Tsuda, 2000). Both roots and shoots were cut at distance of 2 cm from the junction points. Then the shoot was connected to a tube designed to perfuse water into the base of the shoot with stepwise increasing pressures. Twenty minutes after applying a given pressure, the volume of water that passed through each root type (length of ca. 2 cm) was determined by weighing a soft tissue before and ten minutes after absorbing water from cut end of roots. The outflow from each root segment was collected in a separate soft tissue placed in a vertex tip. The slope of the linear regression of flow rate plotted against the applied pressure yielded the axial conductance of the root segment. Four to five replicates were taken for these experiments. Note that the axial conductances measured here refer to axial conductance of root-shoot junction of seminal, crown and brace roots at a distance of 58–65 cm, 45–52, and 30–40 cm from root tip, respectively. Here we were constrained to the maximum length of each root type. Fig. 3(b) shows how we adapted the procedure to the root-shoot junction of maize roots.

2.6. Optimization

The objective of the optimization procedure was to obtain the distribution of root radial conductivity "k_r" [$L\,P^{-1}T^{-1}$] along root axes of different root types. First (scenario 1, Table 1), we optimized k_x and k_r based on K_{root} measurements only, assuming that they were unique (uniform values for each root type). In this first scenario, the measurements of k_x were thus not used. In the next scenarios (2–6), we assumed that k_r and k_x were functions of the distance to the tip.

The intrinsic axial conductance profile was independently fitted on k_x measurements, using linear piecewise functions of distance to the tip.

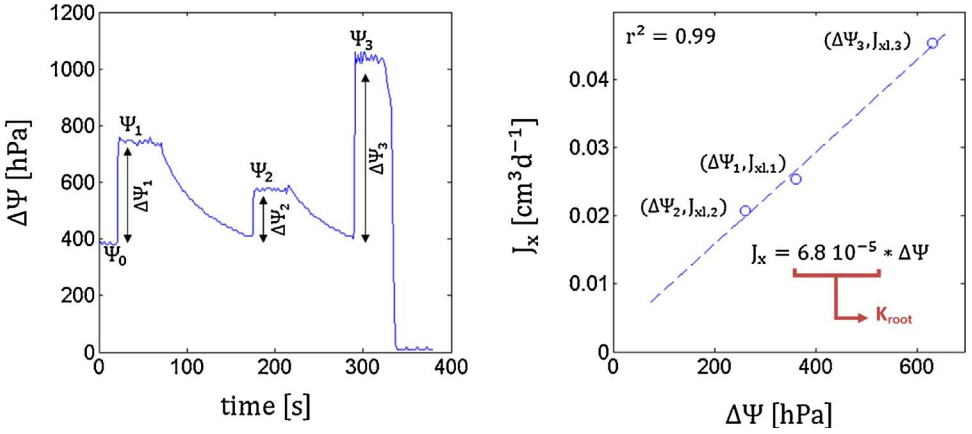

Fig. 2. Example of root total conductance measurement. Left: A series of three successive clamps are applied to a specific root. Right: The corresponding water flow rates are recorded and plotted against the imposed pressure differences. The slope of the linear regression yields the conductance K_{root}.

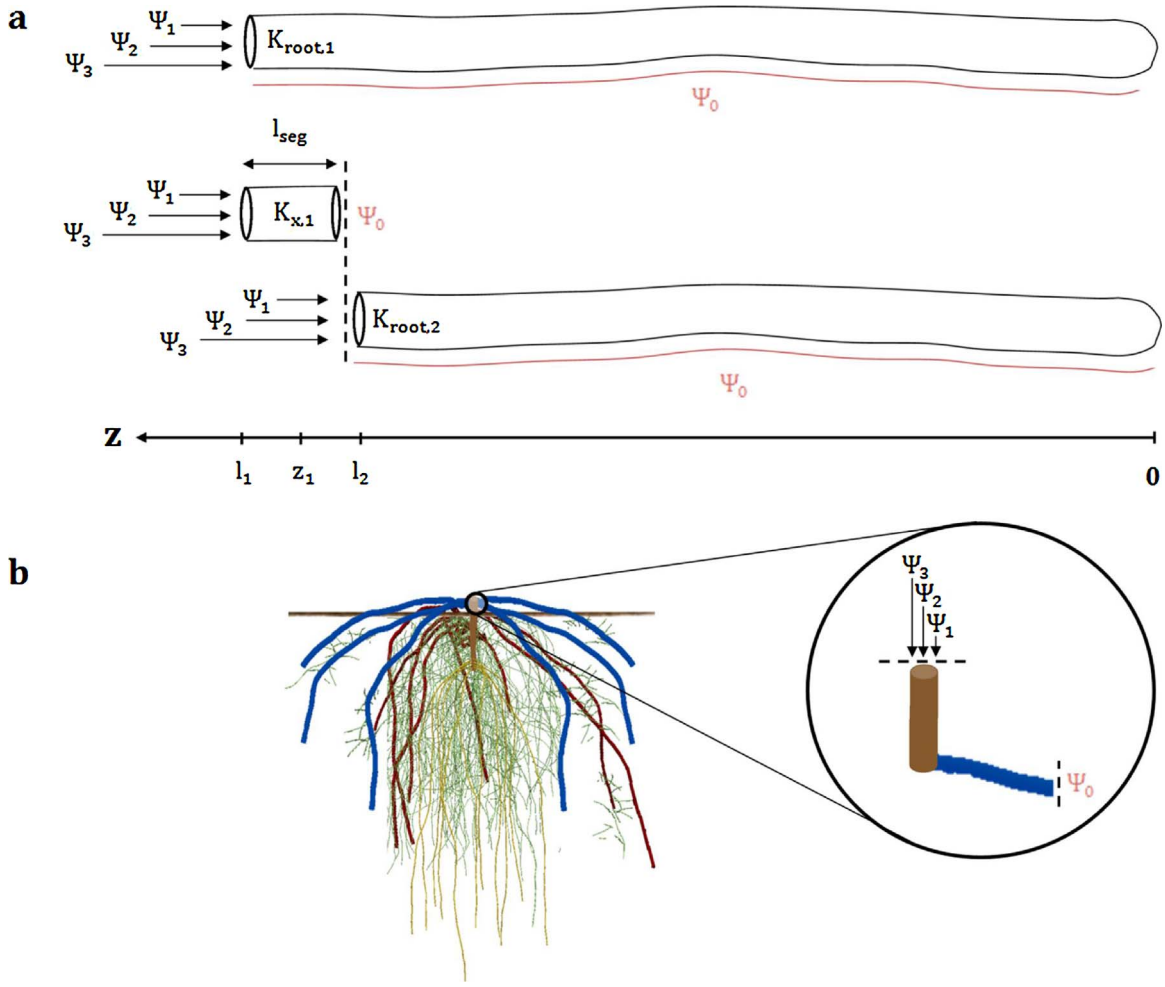

Fig. 3. Schemes of water pressures (equilibrium: Ψ_0, applied: Ψ_1, Ψ_2, Ψ_3) around excised roots during the measurement of their hydraulic conductance. Subplot a: K_{root} is measured for root length 1. A proximal segment is cut off, for which the axial conductance K_x is measured. The measurement of K_{root} is then repeated for root length 2. Subplot b: Zoom on a brace root-shoot junction where the hydraulic conductance is measured.

Various types of functions were then used to optimize profiles of root radial conductivity (scenarios 2–6, Table 1), with the objective of fitting the root total conductance profiles. The chosen indicator of quality of fit was the adjusted r-square, as the total number of model parameters is scenario-dependent. Note that we calculated the adjusted r-square based on the mean value of the repeated observations at each distance from the tip, and not on individual observations.

The five considered k_r functions were: constant, linear, exponential, stepwise (max. 3 steps) and piecewise (max. 5 points). The scenarios were selected for their simplicity, flexibility and their relatively low number of parameters as compared to the number of observations. More information about the chosen distributions is given in Appendix B or in Zarebanadkouki et al. (2016) and in Meunier et al. (2016a). In Table 1, the last column gives the range of total number optimized parameters, which is the sum of the third (number of optimized parameters for the axial conductance) and the fifth (number of optimized parameters for the radial conductivity) columns.

The optimizations were achieved in MATLAB with the Multistart heuristic algorithm OQNLP (Optimal Methods Inc., USA) as global solver. The analytical solutions of Landsberg and Fowkes (1978) and Meunier et al. (2016a) were used to compute analytical solutions of Eq. (A4) (see Appendix A) for scenario 1 and 2–5, respectively.

3. Results

3.1. Conductance results and fits

Good fits (r^2 between 0.95 and 1) were obtained from the regression between the water flow and the pressure transduced by the pressure probe.

Table 1
Summary of the considered scenarios for fitting the measurements.

Scenario	$k_x(z)$ function	$k_x(z)$ parameters	$k_r(z)$ function	$k_r(z)$ parameters	Unknown parameters in K_{root} optimization
1	constant	1	constant	1	2
2	Linear piecewise	4 to 8 (separate fit)	constant	1	5–9
3	Linear piecewise	4 to 8 (separate fit)	Linear	2	6–10
4	Linear piecewise	4 to 8 (separate fit)	exponential	2	6–10
5	Linear piecewise	4 to 8 (separate fit)	stepwise	5	9–13
6	Linear piecewise	4 to 8 (separate fit)	Linear piecewise	6	10–14

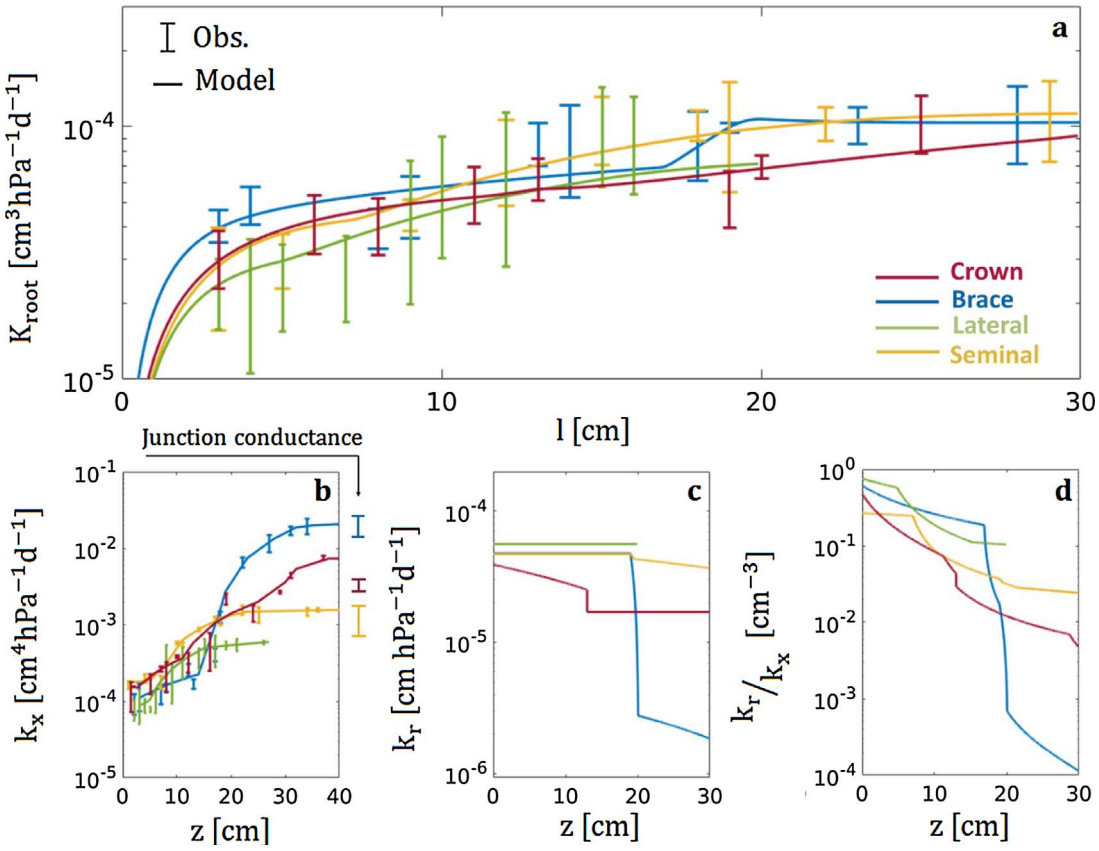

Fig. 4. Hydraulic properties of the different root types of maize. Subplots a and b: total and axial hydraulic conductances of different root types as function of distance from root tip, respectively. Data presented as dots are average of 4–5 measurements and the error bars the standard divisions. Profiles plotted as solid lines are the best profiles obtained from simulation of water flow into unbranched roots of varying length. Subplots c: best fitted profiles of radial conductivity that reproduces measured profiles of total hydraulic conductance. Subplot d: ratio of radial conductivity to axial conductance derived from the analysis along the root axis. In subplot b the junction conductances of the different root types are shown as well.

Fig. 4 shows the profile of hydraulic properties along different root types of maize plant. Subplots 4a and 4b show total and axial hydraulic conductances obtained from root pressure probe measurements, respectively (data presented as dots). Both total and axial hydraulic conductances increase with increasing length or distance from root tip and eventually reach a plateau. After simulation of water flow into unbranched roots of varying length, the profiles of axial conductance and radial conductivity were obtained for each root type (Fig. 4b and c, respectively). Here, for given boundary condition, profiles were optimized to best reproduce the measured profile of total and axial conductance (solid line). The resulting total conductance with the local hydraulic properties are plotted as solid lines in subplot a. The root mean radii were 0.067, 0.052, 0.037, 0.03 and 0.042 for brace, crown, seminal, maize lateral and lupine lateral roots, respectively. Note that the brace roots data were already presented in Meunier et al. (2016a).

Then the ratio of root axial conductance and radial conductivity along the root axis is plotted in subplot 4d. Throughout the whole manuscript, we keep the same colours that represent the different root types. Note that the units used in this study for length, time and pressure are centimetre, day and hectopascal respectively, consistently with the study of Couvreur et al. (2014) for example.

As shown in subplots b and c, the axial conductance and the radial conductivity are increasing and decreasing, respectively, in all maize root types. It leads to an increasing total root conductance for all root types (subplot a) and a decreasing ratio of radial conductivity to axial conductance (subplot d). Surprisingly, the axial conductance is the largest for the brace roots which reveals a potential important role for root water uptake despite the fact that these roots come quite late during plant development and probably have access to a limited amount of water. This could be due to the fact that no water stress was applied during the experiment.

From subplot d, it is clear that conductivities ratios are noticeably different in maize roots. This is of course due to the differences of axial conductances (subplot b) and radial conductivities (subplot c). Around 15 cm from the tip for example, brace roots display a ratio ten times larger than crown roots, mainly because of their larger radial conductivity.

Similarly, hydraulic properties of lateral roots of lupine are represented in Fig. 5. The y-axis limits have been kept the same as the ones presented in Fig. 4 to easily compare the absolute values of measurements between the two species. Similarly to the results obtained for the maize roots, the axial conductance is increasing with distance from the tip, while the best scenario for radial conductivity is the constant one. As a consequence, the lupine total root conductance is strictly increasing (Meunier et al., 2017) and the ratio of radial conductivity to axial conductance strictly decreasing."

Finally, the axial conductances of root-shoot junction of three main maize root types were measured. We obtained (0.0089 ± 0.0026) cm^3 $hPa^{-1}d^{-1}$, (0.0015 ± 0.00025) cm^3 $hPa^{-1}d^{-1}$ and (0.00054 ± 0.00025) cm^3 $hPa^{-1}d^{-1}$ for brace, crown and seminal roots respectively. These axial conductances refer to axial conductance of root-shoot junction of seminal, crown and brace roots at a distance of 58–65 cm, 45–52, and 30–40 cm from root tip, respectively.

The brace roots have the largest axial hydraulic conductance and the seminal roots have the smallest. Axial hydraulic conductances of brace roots are 11.46 times larger than the ones of crown roots which are, in turn 2.79 times larger than the ones of seminal roots. The brace roots have a significantly better junction to the shoot (ANOVA test,

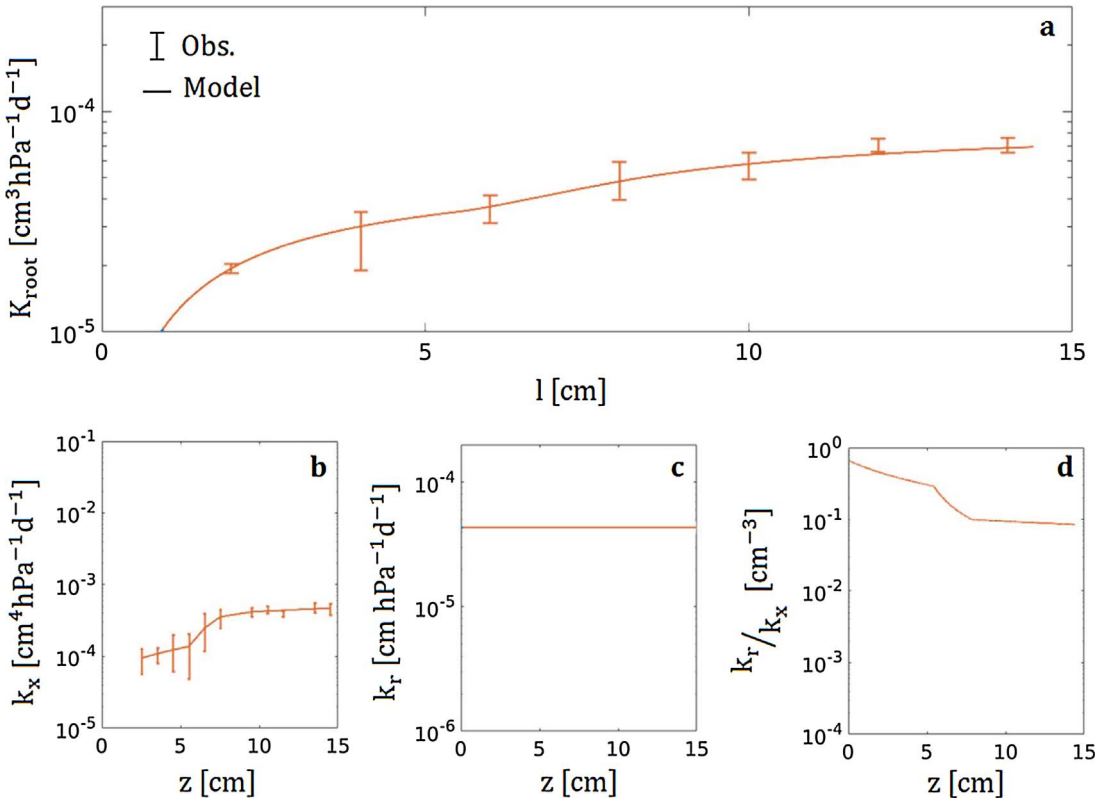

Fig. 5. Hydraulic properties of the lateral roots of lupine. Subplots a and b: total and axial hydraulic conductance of different root types as function of distance from root tip, respectively. Data presented as dots are average of 3–7 measurements and the error bars the standard divisions. Profiles plotted as solid lines are the best profiles obtained from simulation of water flow into unbranched roots of varying length. Subplots c: best fitted profiles of radial conductivity that reproduces measured profiles of total hydraulic conductance. Subplot d: ratio of radial conductivity to axial conductance derived from the analysis along the root axis.

$p < 0.01$), than the two order main root types.

3.2. Quality of fit

The corresponding hydraulic (axial and radial) functions are given in tables of Appendix C in the form of conductivity/position couples for both species and all root types. The adjusted correlation coefficients for best scenarios are indicated as well. They are all satisfactory higher for the best fit of axial conductance profiles (0.93–0.99) and lower for the best fit of radial conductivity profile (0.65–0.97). For the latter, the scenario 4 is always privileged except for the maize and lupine lateral roots where the constant radial conductivity profile reached the highest adjusted r-square for both species.

The measurements and fittings are represented all together in Fig. 6 for both the axial conductances (bottom) and the total conductances (top). The two general cases may be compared in terms of quality of fits: the scatter plot represent the fitted scenario 0 and the crosses, the best fitted function between the four other scenarios (1–4). The two simulation sets reach similar fitting quality for the root total conductance (r-square a little bit larger than 0.8) but have abilities of fitting the axial conductances pretty contrasted. Since several orders of magnitudes of differences were observed between measurements of axial conductances along the root axes, constant scenarios could not catch such a variation with satisfactory fitting.

4. Discussion

Interestingly, the measured total conductances (K_{root}) of different root types and plant species are in the same order of magnitude (see Figs. 4 and 5, top). More strikingly, the evolutions of K_{root} as a function of root length are also generally similar (Fig. 4a). As expected (see Meunier et al., 2017; Meunier et al., 2016a), a plateau of maximal conductance is reached as the root grows.

The obtained value corresponds to an uptake of 1 cm^3d^{-1} per mature root for a pressure difference of 1 MPa, which makes sense we compare the total transpiration of the plant and the total numbers of roots observed. In contrast measured axial conductances differ significantly (Fig. 6, bottom: more than two orders of magnitudes between the smallest and largest measurements). The latter result is expected when comparing roots of different orders and ages, the former is surprising. The lupine root conductances are in average smaller but the measurements correspond to smaller lateral root diameters. When compared, the lateral roots of the two species are rather similar (r^2 of 0.85) and the best fits were both obtained with homogeneous radial conductivity functions. As a consequence the radial profiles of hydraulic conductivity are similar between the species.

In Fig. 7, we plotted the Standard Uptake Density (SUD, i.e. the longitudinal profile of relative water uptake per unit root length in conditions of homogeneous water potential at root surface, see Meunier et al. (2017)) for the different root types. They were calculated using a single root scenario just as in Zarebanadkouki et al. (2016). These results were further integrated to derive a cumulative fraction of the relative water uptake along the different root types (subplots b and d). These curves represent the cumulated percentage of water taken up between the root tip and any position z along the root axis.

As illustrated by the bottom line of Fig. 7, except for the brace root, most of the water is taken up by the distal region (close to the shoot or the mother root junction). This result is similar to the experimental observation of Sanderson (1983) in barley. For brace, crown seminal and lateral roots of maize, the half root close to the root tip takes up to 92%, 33%, 18% and 35% of the water taken up by the whole root, respectively. Similarly for lupine lateral roots, only 35% of the water is taken up by the half root closer to the root tip. For the principal roots of maize, at least 80% of the water is taken up in the first 35 cm of the

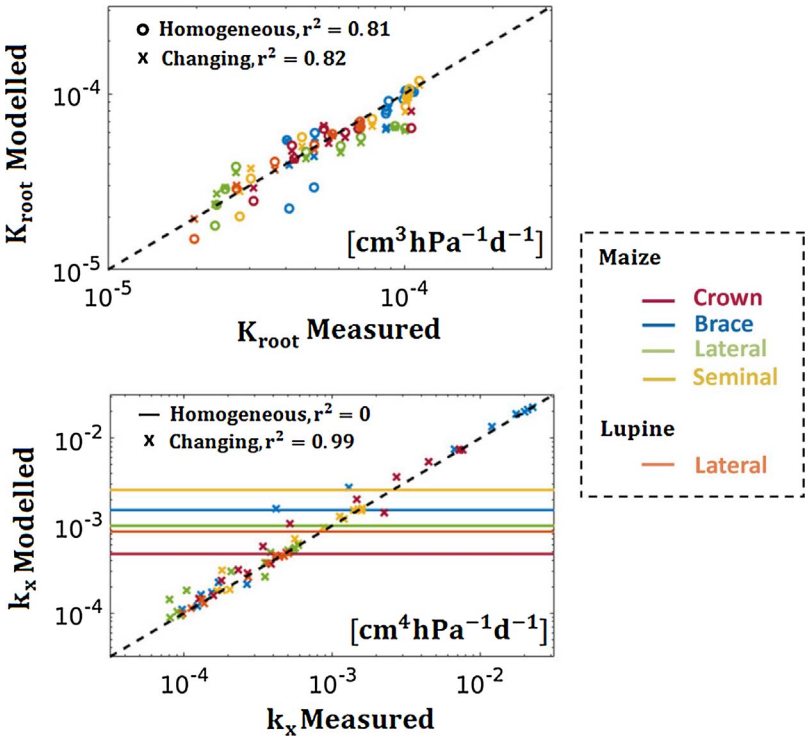

Fig. 6. Overall quality of fits for the root total conductances (top) and the axial conductance (bottom). Scenario 1 (circles and lines) and best scenario (crosses) are compared in terms of correlation coefficient.

roots. This suggests that after the 35 cm then the root length is mainly used to conduct water and not to take it up anymore.

From empirical observations reported in the literature, the opening of early metaxylem vessels progressively occurs in the region from 4 to beyond 14 cm from the root tip in maize (Frensch and Steudle, 1989; Wenzel et al., 1989). Our measurements suggest that the timing of early metaxylem vessels opening varies among root types. In brace roots, the dramatic increase of root axial conductance related to early metaxylem opening took place in the narrow range between 15 and 25 cm from the apex. In contrast, our observations suggest that in crown roots early metaxylem vessels start opening closer to the root tip and new vessels of that type keep on reaching maturity beyond 30 cm from the apex.

Late metaxylem vessels reportedly reach maturity 40–50 cm from the root tip in maize, increasing the axial conductance by an extra order of magnitude (Doussan et al., 1998a; St. Aubin et al., 1986), and thus were likely not open in our root samples.

Regarding the root-shoot junction conductances, it must be said that cellulosic diaphragms, or "pit membranes", that separate a branch from its mother root xylem vessels were reported to filter out particles as small as 5 nm (Shane, 2000), like common primary cellulosic walls (hydraulic conductivity: 7 10^{-3} $m^2s^{-1}MPa^{-1}$ (Steudle and Boyer, 1985)). Assuming 50 × 50 µm connective xylem junction surface, and 1 µm thick diaphragms (Shane, 2000), yields a junction hydraulic conductance of 1.7 10^{-3} $cm^3d^{-1}hPa^{-1}$, which corresponds to the range measured in our crown roots. Corresponding anatomical analyses for brace roots were not documented in the literature. The higher

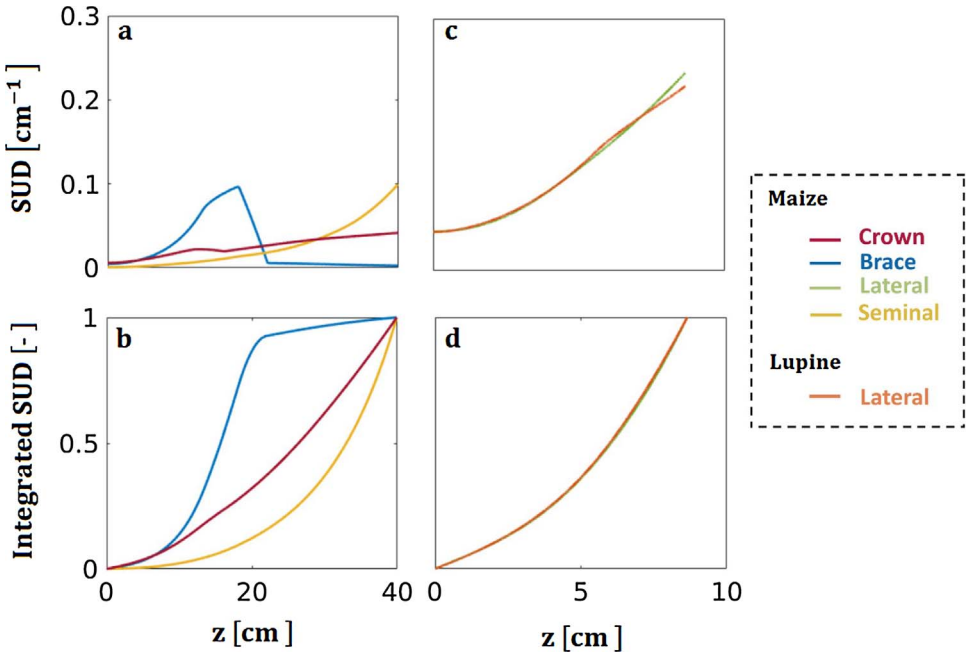

Fig. 7. Standard Uptake Density (i.e. relative water uptake along longitudinal axis) in the different maize and lupine root types (top, subplots a and c); Integrated Standard Uptake Density (i.e. integral of SUD along the longitudinal root axis) in the different maize and lupine root types (bottom, subplots b and d).

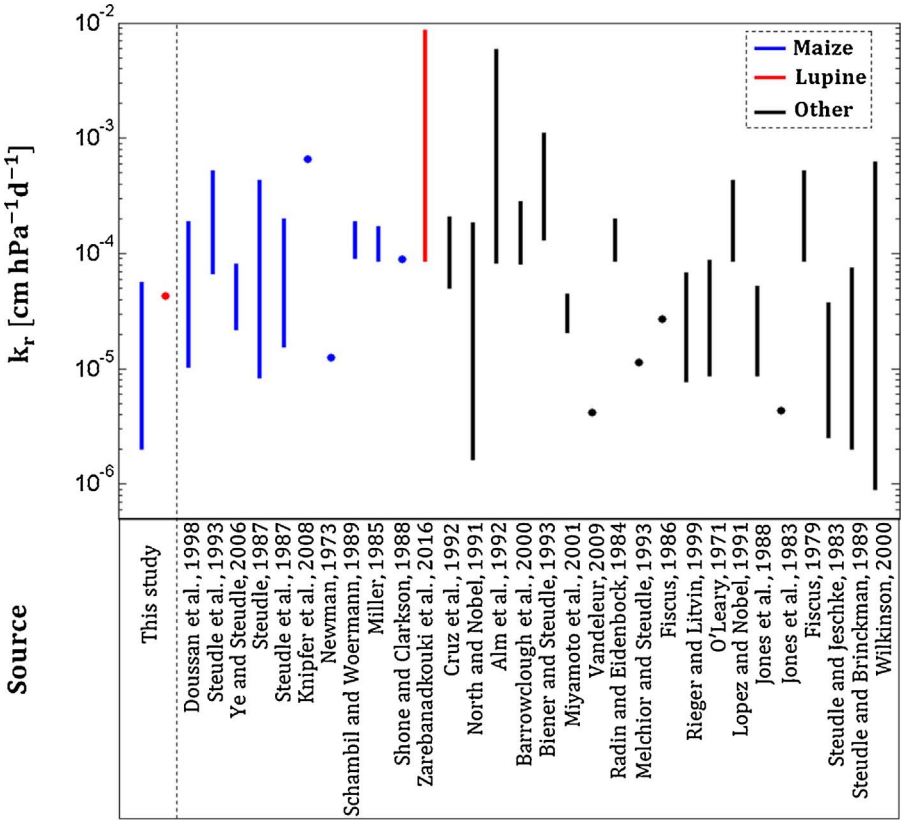

Fig. 8. Comparison of the root radial conductivity obtained in this study and the ones measured in the literature for maize (blue), lupine (red) and other herbaceous species (black). (For interpretation of the references to colour in this figure legend, the reader is referred to the web version of this article.)

junction conductance of brace roots might for instance be due to larger pore size in junction diaphragms as reported in the literature for various plants (Sperry and Tyree, 1988; Van Alfen et al., 1983).

The optimized root radial conductivities (k_r) tended to decrease with distance from the tip in principal roots, and remained stable in laterals. Longitudinal variations of k_r were not always observed in maize principal roots (e.g. (Frensch et al., 1996)). In cases they were, anatomical features such as the systematic development of hydrophobic barriers (Tylová et al., 2017) and aerenchyma were considered responsible for the k_r spatial gradient (Doussan et al., 1998a; Fan et al., 2007). Cell plasma membrane permeability was reported not to vary longitudinally (Zimmermann et al., 2000) and would thus not contribute to k_r variations.

Maize laterals systematically form an endodermal Casparian strip, but the development of other apoplastic barriers remains quite limited when grown in well-watered soil (Tylová et al., 2017), which may explain why we do not observe variations of k_r along laterals (Fig. 5). The longitudinal k_r gradients previously observed in lupine laterals (Zarebanadkouki et al., 2016) may be the result of the sandy growth media that is prone to generate water stress and foster the development of suberin lamellae in both endodermis and exodermis, as demonstrated experimentally in maize laterals by Tylová et al. (2017).

In order to evaluate the radial and axial root hydraulic properties derived from the pressure probe experiments, we compared them to root radial and axial conductivities from the literature (Figs. 8 and 9, see Appendix D for references). In these graphs, all the studies are sourced in the bottom panels and the colours correspond to the plant species: blue for maize plant (any genotype), red for lupine (any genotype) and black for other herbaceous species. Most of the presented values of Fig. 8 come from the reviews of Draye et al. (2010) and Rieger and Litvin (1999).

Bars indicate ranges of variation observed in the corresponding studies. The range of radial conductivity observations covers four

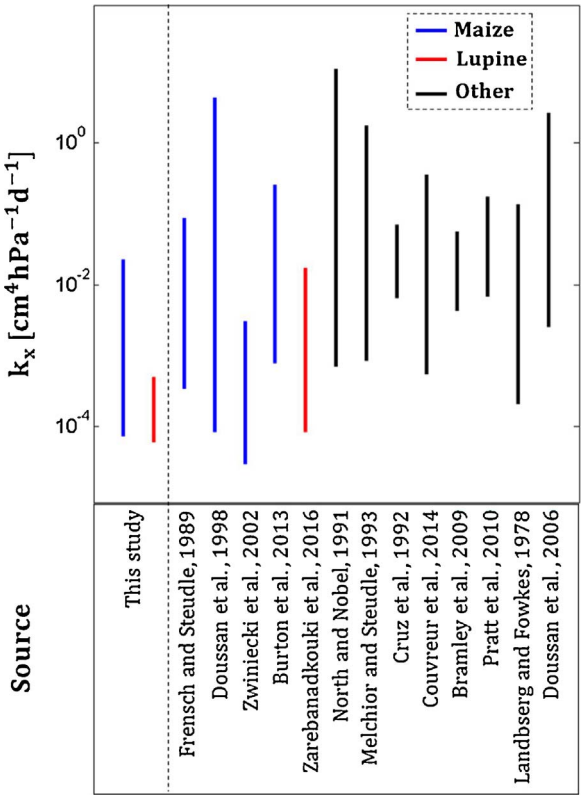

Fig. 9. Comparison of the root axial conductance obtained in this study and the ones measured in the literature for maize (blue), lupine (red) and other herbaceous species (black). (For interpretation of the references to colour in this figure legend, the reader is referred to the web version of this article.)

orders of magnitude (see Fig. 7). The k_r values in our study are rather low as compared to other values for the same species, but correspond on average to observed radial conductivity values of herbaceous plants. The lower limit of the range observed in this study is due to proximal segments of brace roots that were not included in other studies, because too low and not influencing water uptake.

Root conductance (K_{root}) is frequently assumed to be a linear function of root length for sake of simplicity (Ehlert et al., 2009; Hachez et al., 2012). Here we show empirically that the K_{root}(length) function saturates for all of the considered root types, which was demonstrated theoretically to be a consequence of axial hydraulic limitation (Meunier et al., 2017). Hence the typical empirical assumption that k_r is the measured K_{root} per unit root surface could generate substantial bias (underestimation of k_r), particularly for long roots.

More than five orders of magnitudes difference exist between the lowest and highest observed root axial conductances, even in herbaceous species (see Fig. 9). Including woody plants would have further enlarged this range. Again, the axial conductances obtained from our experiments are in the overall range of non-woody species even though they are rather equivalent to the lowest values of the corresponding species.

In our study, it was systematically impossible to fit simultaneously the root axial and total conductances with uniform hydraulic functions. While pretty good results can be obtained for root total conductances alone (see Fig. 7, top), axial measurements highlighted the xylem conductivity changes while the roots grow and develop. It indicates that measuring root conductances with different root lengths is not sufficient to successfully reproduce the conductivity profiles along the roots: it would have been impossible to discriminate a constant hydraulic model from complex ones from these measurements only. The combination of axial and root total conductances only allows one to do so.

When comparing the root-shoot junction conductances with the axial conductances measured from the root tips (the former must be multiplied by the sample length, i.e. around 2 cm, see Fig. 4b), we see that only for the crown roots different values appear, with a probably large water flow reduction due to this bad junction issue. For both the brace and the seminal roots, the junction hydraulic conductivity is similar to the axial conductivity of the corresponding roots close to this point. It suggests a potential plant regulation mechanism for root water uptake location.

All together the measurements derived from this study give a complete description of the hydraulic properties of the maize plant. Combined with architectural properties, it allows building root system hydraulic architecture models fully parametrized that would tackle open questions such as root water uptake distribution in growing root systems and relative roles of the different root types in contrasted environments. These issues will be further investigated in future studies.

5. Conclusion

Root total and axial conductances of maize and lupine unbranched roots were measured using a pressure probe technique. The methodology allowed us to compute root water flows in single roots under different scenarios of radial and axial hydraulic conductivity profiles. The best scenarios fitted the measurements pretty well for both axial (r-square between 0.93 and 0.99) and total (r-square between 0.65 and 0.99) conductances. While the axial properties revealed significant differences between root types and species, the root total conductances were rather similar which implies changes of root radial conductivity between root order and ages. The analysis showed that the root-shoot junction conductances deeply depended on the maize root type with the highest values for the brace roots. Regulation mechanism for location of root water uptake could be the cause of such contrasts between root types. Comparison with the literature unveiled discrepancies between studies for both radial and axial root properties within and between species. Our results were in the low middle.

Conflict of interest

The authors have no conflict of interest to declare.

Acknowledgements

F.M. is supported by “Fonds National de la Recherche Scientifique” of Belgium (FNRS) as Research Fellow and is grateful to this fund for its support. This work was also supported by the Belgian French community ARC 16/21-075 project. V.C. was supported by a post-doctoral grant on the PAI MARS P7/29 project.

Appendix A. Water flow equation in roots

The local root water uptake in a cylindrical root of radius r [L] and length l [L] is usually represented by a membrane-like conceptual model (Landsberg and Fowkes, 1978). The radial flow of water per root length $q_r[L^3L^{-1}T^{-1}]$along the root axis z [L] is driven by the water potential difference between the xylem vessels and the soil-root interface, hereafter referred to as $\Psi_x[P]$ and $\Psi_0[P]$, respectively. It depends also on the inherent radial conductivity of the root tissues $k_r[LP^{-1}T^{-1}]$:

$$q_r(z) = -2\pi r k_r(z)(\Psi_x(z) - \Psi_0) \tag{A1}$$

All the state variables here may vary along the root axis except for the soil-root interface potential that is considered as uniform because in our experiments the roots were entirely immersed in the same water solution. The root axial flow $J_x[L^3T^{-1}]$ that takes place within the xylem vessels is driven by the water potential gradient in these conduits and is regulated by their axial conductance $k_x[L^4P^{-1}T^{-1}]$:

$$J_x(z) = -k_x(z)\frac{d\Psi_x(z)}{dz} \tag{A2}$$

Mass conservation implies that the radial flux as described by Eq. (A1) leads to incremental changes of the axial flow given by Eq. (A2):

$$\frac{d}{dz}J_x(z) = q_r(z) \tag{A2}$$

Combining Eqs. (A1)–(A3) yields the most general form of the water flow equation in an unbranched root in homogeneous soil potential ():

$$\frac{d}{dz}\left(k_x(z)\frac{d\Psi_x(z)}{dz}\right) = 2\pi r k_r(z)(\Psi_x(z) - \Psi_0) \tag{A4}$$

Eq. (A4) is a potentially non-linear differential equation of the second order that can be solved either analytically for several root hydraulic conductivity distribution (constant, linear, exponential or any complex combination of these three functions (Meunier et al., 2016a,b) or numerically for any complex shape of root hydraulic properties (Alm et al., 1992; Doussan et al., 1998b). Solving Eq. (A4) requires two boundary conditions. Here we consider the case of a constant water potential applied at the proximal end (z = l), $\Psi_i[P]$, and a no-flux at the distal root end (z = 0):

$$\begin{cases} J_x(z=0) = 0 \\ \Psi_x(z=l) = \Psi_i \end{cases} \tag{A5}$$

The solution of Eq. (A4) with particular boundary conditions A5 to the xylem potential distribution Ψ_x that, in turn, provides the radial flux and axial flow along the root axis through Eqs. (A1) and (A2), respectively. The water flow can be written as:

$$J_x(l) = K_{root}(\Psi_0 - \Psi_i) = K_{root}\Delta\Psi_i \tag{A6}$$

with K_{root} [$L^3P^{-1}T^{-1}$] being the root total conductance and $\Delta\Psi_i = (\Psi_0 - \Psi_i)$.

When the root is cut, the methodology (pressure clamps and flow measurements) is also applied to the short root segment to compute the axial conductance. For short excised root segments of length l_{seg}[L], we can neglect the radial flow and consider that the root hydraulic properties are homogeneous, Eq. (A4) becomes.

$$\frac{d^2\Psi_x(z)}{dz^2} = 0 \tag{A7}$$

That, solved with the following boundary conditions,

$$\begin{cases} \Psi_x(z=0) = \Psi_0 \\ \Psi_x(z=l_{seg}) = \Psi_i \end{cases} \tag{A8}$$

it leads to the solution:

$$J_x(l_{seg}) = \frac{k_x}{l_{seg}}\Delta\Psi_i = K_x\Delta\Psi_i \tag{A9}$$

where we noted $K_x = \frac{k_x}{l_{seg}}$.

Appendix B. Hydraulic conductivity functions

In this section, we used five kinds of functions to fit the measurements: constant, linear, exponential, stepwise and linear piecewise functions. They are all illustrated in Fig. B1 except for the trivial constant function. In this figure, corresponding function parameters are indicated as well. The number of parameters depends on the number of steps and points for the stepwise and the linear functions. Subplots 3 and 4 are plotted for 2 steps and 2 points, respectively.

Corresponding formula are noted in Eqs. (B1), (B2), (B3) and (B4), respectively.

$$k = k_0 + az \tag{B1}$$

$$k = k_0 exp(az) \tag{B2}$$

$$k = \begin{cases} k_0, z \le z_1 \\ k_1, z > z_1 \end{cases} \tag{B3}$$

$$k = \begin{cases} k_0 + \left(\frac{k_1 - k_0}{z_1}\right)z, z \le z_1 \\ k_1 + \left(\frac{k_2 - k_1}{z_2 - z_1}\right)z - z_1, z > z_1 and\ z \le z_2 \\ k_2 + \left(\frac{k_3 - k_2}{z_3 - z_2}\right)z - z_2, z > z_2 \end{cases} \tag{B4}$$

For the piecewise functions, initial distance to tip z_0 and final distance to tip z_4 (for two points) are taken as 0 and root length, respectively.

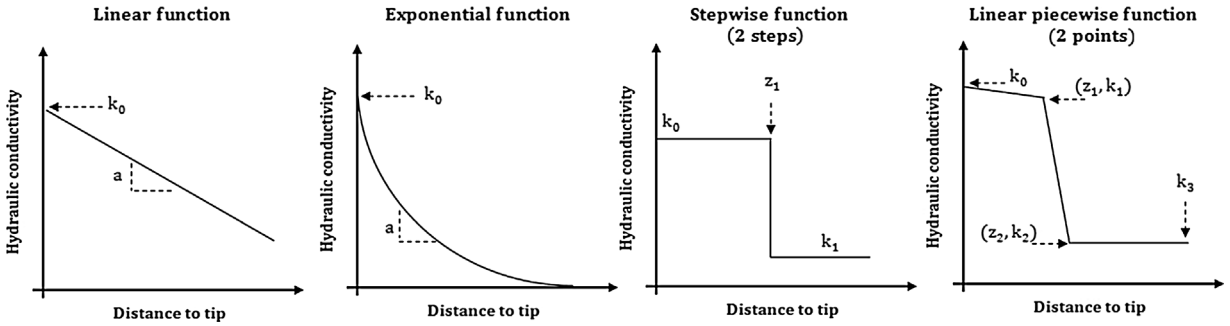

Fig. B1. Illustrations of the analytic functions used in this analysis in addition to the trivial constant function (from left to right, linear, exponential stepwise and linear piecewise functions). Parameters of corresponding functions are indicated as well.

Appendix C. Best fit values

See Tables C1 and C2

Table C1
best fit for the axial conductance profile of maize and lupine roots given as distance from root tip, axial conductance couples. The hydraulic functions were optimized as piecewise functions. The coefficients of determination are given as well for each root type.

Species	Root type	Best scenario	z [cm]	k_x [10^{-4} cm^4 hPa^{-1} d^{-1}]	r^2
Maize	Seminal	4-linear piecewise	0 – 7 – 10 – 21 – 40	1.76 – 1.91 – 5.45 – 14.85 – 15.85	0.98
	Crown	4-linear piecewise	0 – 11.2 – 28.7 – 34.3 – 40	0.82 – 3.71 – 24.44 – 73.63 – 73.63	0.97
	Brace	4-linear piecewise	0 – 16.9 – 27 – 32.6 – 40	0.78 – 2.56 – 121.8 – 195.6 – 225.3	0.99
	Lateral	3-linear piecewise	0 – 4.8 –15.2 – 30	0.74 – 0.98 – 5.04 – 5.99	0.93
Lupine	Lateral	3-linear piecewise	0 – 5.5 – 7.92 – 15	0.62 – 1.44 – 4.22 – 4.95	0.99

Table C2
best fit for the radial conductivity profile of maize and lupine roots given as pairs of distance from root tip and radial conductivity values. The adjusted r-square are provided as well for each root type.

Species	Root type	Best scenario	z [cm]	k_r [cm hPa^{-1} d^{-1}]	r^2 adjusted
Maize	Seminal	3-linear piecewise	0 – 19 – 19.5 – 30	(0.47 – 0.47 – 0.43 – 0.28) * 10^{-4}	0.88
	Crown	3-linear piecewise	0 – 13 – 13.1 – 30	(0.39 – 0.25 – 0.17 – 0.17) * 10^{-4}	0.72
	Brace	3-linear piecewise	0 – 19 – 20 – 30	(0.48 – 0.48 – 0.028 – 0.02) * 10^{-4}	0.83
	Lateral	Constant	0 – 15	(5.62 – 5.62) * 10^{-5}	0.65
Lupine	Lateral	Constant	0 – 15	(4.32 – 4.32) * 10^{-5}	0.97

Appendix D. References for the hydraulic conductivity meta-analysis

Short name	Reference
Alm et al. (1992)	Alm, D.M., Cavelier, J., Nobel, P.S., 1992. A Finite-element Model of Radial and Axial Conductivities for Individual Roots: Development and Validation for Two Desert Succulents. Ann. Bot. 69, 87–92.
Barrowclough (2000)	Barrowclough, D.E., 2000. Radial hydraulic conductivity along developing onion roots. J. Exp. Bot. 51, 547–557. https://doi.org/10.1093/jexbot/51.344.547
Bramley et al. (2009)	Bramley, H., Turner, N.C., Turner, D.W., Tyerman, S.D., 2009. Roles of Morphology, Anatomy, and Aquaporins in Determining Contrasting Hydraulic Behavior of Roots. Plant Physiol. 150, 348–364. https://doi.org/10.1104/pp.108.134098
Burton et al. (2013)	Burton, A.L., Brown, K.M., Lynch, J.P., 2013. Phenotypic Diversity of Root Anatomical and Architectural Traits in Species. Crop Sci. 53, 1042. https://doi.org/10.2135/cropsci2012.07.0440
Couvreur et al. (2014)	Couvreur, V., Vanderborght, J., Draye, X., Javaux, M., 2014. Dynamic aspects of soil water availability for isohydric plants: Focus on root hydraulic resistances. Water Resour. Res. 50, 8891–8906. https://doi.org/10.1002/2014WR015608
Cruz et al. (1992)	Cruz, R.T., Jordan, W.R., Drew, M.C., 1992. Structural changes and associated reduction of hydraulic conductance in roots of Sorghum bicolor L. following exposure to water deficit. Plant Physiol. 99, 203–212.
Doussan et al. (1998b)	Doussan, C., Vercambre, G., Pagès, L., 1998. Modelling of the hydraulic architecture of root systems: An integrated approach to water absorption–distribution of axial and radial conductances in maize. Ann. Bot. 81, 225–232.
Doussan et al. (2006)	Doussan, C., Pierret, A., Garrigues, E., Pagès, L., 2006. Water uptake by plant roots: II–Modelling of water transfer in the soil root-system with explicit account of flow within the root system–Comparison with experiments. Plant Soil 283, 99–117.
Fiscus (1986)	Fiscus, E.L., 1986. Diurnal Changes in Volume and Solute Transport Coefficients of Phaseolus Roots. Plant Physiol. 80, 752–759. https://doi.org/10.1104/pp.80.3.752
Frensch and Steudle (1989)	Frensch, J., Steudle, E., 1989. Axial and radial hydraulic resistance to roots of maize (Zea mays L.). Plant Physiol. 91, 719–726.
Jones et al. (1983)	Jones, H., Tomos, A.D., Leigh, R.A., Jones, R.G.W., 1983. Water-relation parameters of epidermal and cortical cells in the primary root of Triticum aestivum L. Planta 158, 230–236.
Jones et al. (1988)	Jones, H., Leigh, R.A., Jones, R.G.W., Tomos, A.D., 1988. The integration of whole-root and cellular hydraulic conductivities in cereal roots. Planta 174, 1–7.
Knipfer and Steudle (2008)	Knipfer, T., Steudle, E., 2008. Root hydraulic conductivity measured by pressure clamp is substantially affected by internal unstirred layers. J. Exp. Bot. 59, 2071–2084. https://doi.org/10.1093/jxb/ern064
Landsberg and Fowkes (1978)	Landsberg, J.J., Fowkes, N.D., 1978. Water Movement Through Plant Roots. Ann. Bot. 42, 493–508. https://doi.org/10.1093/oxfordjournals.aob.a085488
Lopez and Nobel (1991)	Lopez, F.B., Nobel, P.S., 1991. Root Hydraulic Conductivity of Two Cactus Species in Relation to Root Age, Temperature, and Soil Water Status. J. Exp. Bot. 42, 143–149. https://doi.org/10.1093/jxb/42.2.143

Markhart et al. (1979) Markhart, A.H., Fiscus, E.L., Naylor, A.W., Kramer, P.J., 1979. Effect of Abscisic Acid on Root Hydraulic Conductivity. Plant Physiol. 64, 611–614. https://doi.org/10.1104/pp.64.4.611

Melchior and Steudle (1993) Melchior, W., Steudle, E., 1993. Water Transport in Onion (Allium cepa L.) Roots (Changes of Axial and Radial Hydraulic Conductivities during Root Development). Plant Physiol. 101, 1305–1315. https://doi.org/10.1104/pp.101.4.1305

Miller (1985) Miller, D.M., 1985. Studies of Root Function in Zea mays: IV. Effects of Applied Pressure on the Hydraulic Conductivity and Volume Flow through the Excised Root. PLANT Physiol. 77, 168–174. https://doi.org/10.1104/pp.77.1.168

Miyamoto et al. (2001) Miyamoto, N., Steudle, E., Hirasawa, T., Lafitte, R., 2001. Hydraulic conductivity of rice roots. J. Exp. Bot. 52, 1835–1846. https://doi.org/10.1093/jexbot/52.362.1835

Newman (1973) Newman, E.I., 1973. Permeability to water of the roots of five herbaceous species. New Phytol. 72, 547–555. https://doi.org/10.1111/j.1469-8137.1973.tb04406.x

North and Nobel (1991) North, G.B., Nobel, P.S., 1991. Changes in Hydraulic Conductivity and Anatomy Caused by Drying and Rewetting Roots of Agave deserti (Agavaceae). Am. J. Bot. 78, 906–915. https://doi.org/10.2307/2445169

O'Leary (1974) O'Leary, J.W., 1974. Salinity induced changes in hydraulic conductivity of roots.

Pratt et al. (2010) Pratt, R.B., North, G.B., Jacobsen, A.L., Ewers, F.W., Davis, S.D., 2010. Xylem root and shoot hydraulics is linked to life history type in chaparral seedlings. Funct. Ecol. 24, 70–81. https://doi.org/10.1111/j.1365-2435.2009.01613.x

Radin and Eidenbock (1984) Radin, J.W., Eidenbock, M.P., 1984. Hydraulic Conductance as a Factor Limiting Leaf Expansion of Phosphorus-Deficient Cotton Plants. PLANT Physiol. 75, 372–377. https://doi.org/10.1104/pp.75.2.372

Rieger and Litvin (1999) Rieger, M., Litvin, P., 1999. Root system hydraulic conductivity in species with contrasting root anatomy. J. Exp. Bot. 50, 201–209. https://doi.org/10.1093/jxb/50.331.201

Schambil and Woermann (1989) Schambil, F., Woermann, D., 1989. Radial transport of water across cortical sleeves of excised roots of Zea mays L. Planta 178, 488–494.

Shone and Clarkson (1988) Shone, M.G.T., Clarkson, D.T., 1988. Rectification of radial water flow in the hypodermis of nodal roots of Zea mays. Plant Soil 111, 223–229.

Steudle (1994) Steudle, E., 1994. Water transport across roots. Plant Soil 167, 79–90.

Steudle and Brinckmann (1989) Steudle, E., Brinckmann, E., 1989. The Osmometer Model of the Root: Water and Solute Relations of Roots of *Phaseolus coccineus*. Bot. Acta 102, 85–95. https://doi.org/10.1111/j.1438-8677.1989.tb00071.x

Steudle and Jeschke (1983) Steudle, E., Jeschke, W.D., 1983. Water transport in barley roots: Measurements of root pressure and hydraulic conductivity of roots in parallel with turgor and hydraulic conductivity of root cells. Planta 158, 237–248. https://doi.org/10.1007/BF01075260

Steudle et al. (1987) Steudle, E., Oren, R., Schulze, E.-D., 1987. Water transport in maize roots measurement of hydraulic conductivity, solute permeability, and of reflection coefficients of excised roots using the root pressure probe. Plant Physiol. 84, 1220–1232.

Steudle et al. (1993) Steudle, E., Murrmann, M., Peterson, C.A., 1993. Transport of water and solutes across maize roots modified by puncturing the endodermis (further evidence for the composite transport model of the root). Plant Physiol. 103, 335–349.

Vandeleur et al. (2009) Vandeleur, R.K., Mayo, G., Shelden, M.C., Gilliham, M., Kaiser, B.N., Tyerman, S.D., 2009. The Role of Plasma Membrane Intrinsic Protein Aquaporins in Water Transport through Roots: Diurnal and Drought Stress Responses Reveal Different Strategies between Isohydric and Anisohydric Cultivars of Grapevine. Plant Physiol. 149, 445–460.

Wilkinson (2000) Wilkinson, R.E. (Ed.), 2000. Plant-environment interactions, 2nd ed. ed, Books in soils, plants, and the environment. Marcel Dekker, New York.

Ye and Steudle (2006) Ye, Q., Steudle, E., 2006. Oxidative gating of water channels (aquaporins) in corn roots. Plant Cell Environ. 29, 459–470. https://doi.org/10.1111/j.1365-3040.2005.01423.x

Zarebanadkouki et al. (2016) Zarebanadkouki, M., Meunier, F., Couvreur, V., Cesar, J., Javaux, M., Carminati, A., 2016. Estimation of the hydraulic conductivities of lupine roots by inverse modelling of high-resolution measurements of root water uptake. Ann. Bot. mcw154. https://doi.org/10.1093/aob/mcw154

Zwieniecki et al. (2002) Zwieniecki, M.A., Thompson, M.V., Holbrook, N.M., 2002. Understanding the Hydraulics of Porous Pipes: Tradeoffs Between Water Uptake and Root Length Utilization. J. Plant Growth Regul. 21, 315–323. https://doi.org/10.1007/s00344-003-0008-9

References

Ahmed, M.A., Zarebanadkouki, M., Kaestner, A., Carminati, A., 2016. Measurements of water uptake of maize roots: the key function of lateral roots. Plant Soil 398, 59–77. http://dx.doi.org/10.1007/s11104-015-2639-6.

Alm, D.M., Cavelier, J., Nobel, P.S., 1992. A finite-element model of radial and axial conductivities for individual roots: development and validation for two desert succulents. Ann. Bot. 69, 87–92.

Barrowclough, D.E., 2000. Radial hydraulic conductivity along developing onion roots. J. Exp. Bot. 51, 547–557. http://dx.doi.org/10.1093/jexbot/51.344.547.

Bramley, H., Turner, N.C., Turner, D.W., Tyerman, S.D., 2009. Roles of morphology anatomy, and aquaporins in determining contrasting hydraulic behavior of roots. Plant Physiol. 150, 348–364. http://dx.doi.org/10.1104/pp.108.134098.

Burton, A.L., Brown, K.M., Lynch, J.P., 2013. Phenotypic diversity of root anatomical and architectural traits in species. Crop Sci. 53, 1042. http://dx.doi.org/10.2135/cropsci2012.07.0440.

Cattivelli, L., Rizza, F., Badeck, F.-W., Mazzucotelli, E., Mastrangelo, A.M., Francia, E., Marè, C., Tondelli, A., Stanca, A.M., 2008. Drought tolerance improvement in crop plants: an integrated view from breeding to genomics. Field Crops Res. 105, 1–14. http://dx.doi.org/10.1016/j.fcr.2007.07.004.

Comas, L.H., Becker, S.R., Cruz, V.M.V., Byrne, P.F., Dierig, D.A., 2013. Root traits contributing to plant productivity under drought. Front. Plant Sci. 4, 442. http://dx.doi.org/10.3389/fpls.2013.00442.

Couvreur, V., Vanderborght, J., Draye, X., Javaux, M., 2014. Dynamic aspects of soil water availability for isohydric plants: focus on root hydraulic resistances. Water Resour. Res. 50, 8891–8906. http://dx.doi.org/10.1002/2014WR015608.

Cruz, R.T., Jordan, W.R., Drew, M.C., 1992. Structural changes and associated reduction of hydraulic conductance in roots of Sorghum bicolor L following exposure to water deficit. Plant Physiol. 99, 203–212.

Doussan, C., Pagès, L., Vercambre, G., 1998a. Modelling of the hydraulic architecture of root systems: an integrated approach to water absorption—model description. Ann.

Bot. 81, 213–223. http://dx.doi.org/10.1006/anbo.1997.0540.
Doussan, C., Vercambre, G., Pagès, L., 1998b. Modelling of the hydraulic architecture of root systems: an integrated approach to water absorption—distribution of axial and radial conductances in maize. Ann. Bot. 81, 225–232.
Doussan, C., Pierret, A., Garrigues, E., Pagès, L., 2006. Water uptake by plant roots: II–Modelling of water transfer in the soil root-system with explicit account of flow within the root system–Comparison with experiments. Plant Soil 283, 99–117.
Draye, X., Kim, Y., Lobet, G., Javaux, M., 2010. Model-assisted integration of physiological and environmental constraints affecting the dynamic and spatial patterns of root water uptake from soils. J. Exp. Bot. 61, 2145–2155.
Ehlert, C., Maurel, C., Tardieu, F., Simonneau, T., 2009. Aquaporin-mediated reduction in maize root hydraulic conductivity impacts cell turgor and leaf elongation even without changing transpiration. Plant Physiol. 150, 1093–1104. http://dx.doi.org/10.1104/pp.108.131458.
Fan, M., Bai, R., Zhao, X., Zhang, J., 2007. Aerenchyma formed under phosphorus deficiency contributes to the reduced root hydraulic conductivity in maize roots. J. Integr. Plant Biol. 49, 598–604.
Farooq, M., Wahid, A., Kobayashi, N., Fujita, D., Basra, S.M.A., 2009. Plant drought stress: effects, mechanisms and management. Agron. Sustain. Dev. 29, 185–212. http://dx.doi.org/10.1051/agro:2008021.
Fiscus, E.L., 1986. Diurnal changes in volume and solute transport coefficients of phaseolus roots. Plant Physiol. 80, 752–759. http://dx.doi.org/10.1104/pp.80.3.752.
Frensch, J., Steudle, E., 1989. Axial and radial hydraulic resistance to roots of maize (Zea mays L.). Plant Physiol. 91, 719–726.
Frensch, J., Hsiao, T.C., Steudle, E., 1996. Water and solute transport along developing maize roots. Planta 198, 348–355. http://dx.doi.org/10.1007/BF00620050.
Hachez, C., Veselov, D., Ye, Q., Reinhardt, H., Knipfer, T., Fricke, W., Chaumont, F., 2012. Short-term control of maize cell and root water permeability through plasma membrane aquaporin isoforms: maize root plasma membrane aquaporins. Plant Cell Environ. 35, 185–198. http://dx.doi.org/10.1111/j.1365-3040.2011.02429.x.
Hammer, G.L., Dong, Z., McLean, G., Doherty, A., Messina, C., Schussler, J., Zinselmeier, C., Paszkiewicz, S., Cooper, M., 2009. Can changes in canopy and/or root system architecture explain historical maize yield trends in the U.S. corn belt? Crop Sci. 49, 299. http://dx.doi.org/10.2135/cropsci2008.03.0152.
Javaux, M., Schröder, T., Vanderborght, J., Vereecken, H., 2008. Use of a three-dimensional detailed modeling approach for predicting root water uptake. Vadose Zone J. 7, 1079–1088.
Jones, H., Tomos, A.D., Leigh, R.A., Jones, R.G.W., 1983. Water-relation parameters of epidermal and cortical cells in the primary root of Triticum aestivum L. Planta 158, 230–236.
Jones, H., Leigh, R.A., Jones, R.G.W., Tomos, A.D., 1988. The integration of whole-root and cellular hydraulic conductivities in cereal roots. Planta 174, 1–7.
Knipfer, T., Steudle, E., 2008. Root hydraulic conductivity measured by pressure clamp is substantially affected by internal unstirred layers. J. Exp. Bot. 59, 2071–2084. http://dx.doi.org/10.1093/jxb/ern064.
Landsberg, J.J., Fowkes, N.D., 1978. Water movement through plant roots. Ann. Bot. 42, 493–508. http://dx.doi.org/10.1093/oxfordjournals.aob.a085488.
Leitner, D., Meunier, F., Bodner, G., Javaux, M., Schnepf, A., 2014. Impact of contrasted maize root traits at flowering on water stress tolerance −A simulation study. Field Crops Res. http://dx.doi.org/10.1016/j.fcr.2014.05.009.
Lobet, G., Couvreur, V., Meunier, F., Javaux, M., Draye, X., 2014. Plant water uptake in drying soils. Plant Physiol. http://dx.doi.org/10.1104/pp.113.233486.
Lopez, F.B., Nobel, P.S., 1991. Root hydraulic conductivity of two cactus species in relation to root age temperature, and soil water status. J. Exp. Bot. 42, 143–149. http://dx.doi.org/10.1093/jxb/42.2.143.
Lynch, J.P., Brown, K.M., 2012. New roots for agriculture: exploiting the root phenome. Philos. Trans. R. Soc. B Biol. Sci. 367, 1598–1604.
Lynch, J.P., 2013. Steep, cheap and deep: an ideotype to optimize water and N acquisition by maize root systems. Ann. Bot. http://dx.doi.org/10.1093/aob/mcs293.
Markhart, A.H., Fiscus, E.L., Naylor, A.W., Kramer, P.J., 1979. Effect of abscisic acid on root hydraulic conductivity. Plant Physiol. 64, 611–614. http://dx.doi.org/10.1104/pp.64.4.611.
Martre, P., Durand, J.-L., Cochard, H., 2000. Changes in axial hydraulic conductivity along elongating leaf blades in relation to xylem maturation in tall fescue. New Phytol. 146, 235–247. http://dx.doi.org/10.1046/j.1469-8137.2000.00641.x.
McElrone, A.J., Choat, B., Gambetta, G.A., Brodersen, C.R., 2013. Water uptake and transport in vascular plants. Nat. Educ. Knowl. 5, 6.
Melchior, W., Steudle, E., 1993. Water transport in onion (Allium cepa L.) roots (changes of axial and radial hydraulic conductivities during root development). Plant Physiol. 101, 1305–1315. http://dx.doi.org/10.1104/pp.101.4.1305.
Meunier, F., Couvreur, V., Draye, X., Vanderborght, J., Javaux, M., 2016a. Water movement through plant roots: exact solutions of the water flow equation in roots with varying hydraulic properties. Hydrol. Earth Syst. Sci. Discuss. 1–35. http://dx.doi.org/10.5194/hess-2016-633.
Meunier, F., Javaux, M., Couvreur, V., Draye, X., Javaux, M., Vanderborght, J., Vanderborght, J., 2016b. A new model for optimizing the water acquisition of root hydraulic architectures over full crop cycles. IEEE 140–149. http://dx.doi.org/10.1109/FSPMA.2016.7818300.
Meunier, F., Couvreur, V., Draye, X., Vanderborght, J., Javaux, M., 2017. Towards quantitative root hydraulic phenotyping: novel mathematical functions to calculate plant-scale hydraulic parameters from root system functional and structural traits. J. Math. Biol. http://dx.doi.org/10.1007/s00285-017-1111-z.
Miller, D.M., 1985. Studies of root function in zea mays: IV. Effects of applied pressure on the hydraulic conductivity and volume flow through the excised root. Plant Physiol. 77, 168–174. http://dx.doi.org/10.1104/pp.77.1.168.
Miyamoto, N., Steudle, E., Hirasawa, T., Lafitte, R., 2001. Hydraulic conductivity of rice roots. J. Exp. Bot. 52, 1835–1846. http://dx.doi.org/10.1093/jexbot/52.362.1835.
Newman, E.I., 1973. Permeability to water of the roots of five herbaceous species. New Phytol. 72, 547–555. http://dx.doi.org/10.1111/j.1469-8137.1973.tb04406.x.
North, G.B., Nobel, P.S., 1991. Changes in hydraulic conductivity and anatomy caused by drying and rewetting roots of agave deserti (Agavaceae). Am. J. Bot. 78, 906–915. http://dx.doi.org/10.2307/2445169.
O'Leary, J.W., 1974. Salinity induced changes in hydraulic conductivity of roots. Struct. Funct. Prim. Root Tissues Proc. Symp.
Passioura, J.B., 1980. The transport of water from soil to shoot in wheat seedlings. J. Exp. Bot. 31, 333–345. http://dx.doi.org/10.1093/jxb/31.1.333.
Pratt, R.B., North, G.B., Jacobsen, A.L., Ewers, F.W., Davis, S.D., 2010. Xylem root and shoot hydraulics is linked to life history type in chaparral seedlings. Funct. Ecol. 24, 70–81. http://dx.doi.org/10.1111/j.1365-2435.2009.01613.x.
Radin, J.W., Eidenbock, M.P., 1984. Hydraulic conductance as a factor limiting leaf expansion of phosphorus-deficient cotton plants. Plant Physiol. 75, 372–377. http://dx.doi.org/10.1104/pp.75.2.372.
Rieger, M., Litvin, P., 1999. Root system hydraulic conductivity in species with contrasting root anatomy. J. Exp. Bot. 50, 201–209. http://dx.doi.org/10.1093/jxb/50.331.201.
Sanderson, J., Whitbread, F.C., Clarkson, D.T., 1988. Persistent xylem cross-walls reduce the axial hydraulic conductivity in the apical 20 cm of barley seminal root axes: implications for the driving force for water movement. Plant Cell Environ. 11, 247–256.
Sanderson, J., 1983. Water-uptake by different regions of the barley root − pathways of radial flow in relation to development of the endodermis. J. Exp. Bot. 34, 240–253.
Schambil, F., Woermann, D., 1989. Radial transport of water across cortical sleeves of excised roots of Zea mays L. Planta 178, 488–494.
Schnepf, A., Leitner, D., Landl, M., Lobet, G., Mai, T.H., Morandage, S., Sheng, C., Zoerner, M., Vanderborght, J., Vereecken, H., 2017. CRootBox: A Structural-Functional Modelling Framework For Root Systems. http://dx.doi.org/10.1101/139980.
Schoppach, R., Wauthelet, D., Jeanguenin, L., Sadok, W., 2014. Conservative water use under high evaporative demand associated with smaller root metaxylem and limited trans-membrane water transport in wheat. Funct. Plant Biol. 41, 257. http://dx.doi.org/10.1071/FP13211.
Shane, M., 2000. Architecture of branch-root junctions in maize: structure of the connecting xylem and the porosity of pit membranes. Ann. Bot. 85, 613–624. http://dx.doi.org/10.1006/anbo.2000.1113.
Shone, M.G.T., Clarkson, D.T., 1988. Rectification of radial water flow in the hypodermis of nodal roots ofZea mays. Plant Soil 111, 223–229.
Sperry, J.S., Tyree, M.T., 1988. Mechanism of water stress-induced xylem embolism. Plant Physiol. 88, 581–587. http://dx.doi.org/10.1104/pp.88.3.581.
St. Aubin, G., Canny, M.J., McCully, M.E., 1986. Living vessel elements in the late metaxylem of sheathed maize roots. Ann. Bot. 58, 577–588. http://dx.doi.org/10.1093/annbot/58.4.577.
Steudle, E., Boyer, J.S., 1985. Hydraulic resistance to radial water flow in growing hypocotyl of soybean measured by a new pressure-perfusion technique. Planta 164, 189–200. http://dx.doi.org/10.1007/BF00396081.
Steudle, E., Brinckmann, E., 1989. The osmometer model of the root: water and solute relations of roots of *Phaseolus coccineus*. Bot. Acta 102, 85–95. http://dx.doi.org/10.1111/j.1438-8677.1989.tb00071.x.
Steudle, E., Jeschke, W.D., 1983. Water transport in barley roots: measurements of root pressure and hydraulic conductivity of roots in parallel with turgor and hydraulic conductivity of root cells. Planta 158, 237–248. http://dx.doi.org/10.1007/BF01075260.
Steudle, E., Oren, R., Schulze, E.-D., 1987. Water transport in maize roots measurement of hydraulic conductivity, solute permeability, and of reflection coefficients of excised roots using the root pressure probe. Plant Physiol. 84, 1220–1232.
Steudle, E., Murrmann, M., Peterson, C.A., 1993. Transport of water and solutes across maize roots modified by puncturing the endodermis (further evidence for the composite transport model of the root). Plant Physiol. 103, 335–349.
Steudle, E., 1994. Water transport across roots. Plant Soil 167, 79–90.
Steudle, E., 2000. Water uptake by roots: effects of water deficit. J. Exp. Bot. 51, 1531–1542. http://dx.doi.org/10.1093/jexbot/51.350.1531.
Tardieu, F., Simonneau, T., Parent, B., 2015. Modelling the coordination of the controls of stomatal aperture, transpiration, leaf growth, and abscisic acid: update and extension of the Tardieu-Davies model. J. Exp. Bot. 66, 2227–2237. http://dx.doi.org/10.1093/jxb/erv039.
Tardieu, F., 2012. Any trait or trait-related allele can confer drought tolerance: just design the right drought scenario. J. Exp. Bot. 63, 25–31.
Tsuda, M., 2000. Plant hydraulic conductance measured by the high pressure flow meter in crop plants. J. Exp. Bot. 51, 823–828. http://dx.doi.org/10.1093/jexbot/51.345.823.
Tylová, E., Pecková, E., Blascheová, Z., Soukup, A., 2017. Casparian bands and suberin lamellae in exodermis of lateral roots: an important trait of roots system response to abiotic stress factors. Ann. Bot. 120, 71–85. http://dx.doi.org/10.1093/aob/mcx047.
Vadez, V., 2014. Root hydraulics: the forgotten side of roots in drought adaptation. Field Crops Res. http://dx.doi.org/10.1016/j.fcr.2014.03.017.
Van Alfen, N.K., McMillan, B.D., Turner, V., Hess, W.M., 1983. Role of pit membranes in macromolecule-induced wilt of plants. Plant Physiol. 73, 1020–1023. http://dx.doi.org/10.1104/pp.73.4.1020.
Vandeleur, R.K., Mayo, G., Shelden, M.C., Gilliham, M., Kaiser, B.N., Tyerman, S.D., 2009. The role of plasma membrane intrinsic protein aquaporins in water transport through roots: diurnal and drought stress responses reveal different strategies between isohydric and anisohydric cultivars of grapevine. Plant Physiol. 149, 445–460. http://dx.doi.org/10.1104/pp.108.128645.
Vetterlein, D., Doussan, C., 2016. Root age distribution: how does it matter in plant processes? A focus on water uptake. Plant Soil 407, 145. http://dx.doi.org/10.1007/s11104-016-2849-6.
Wenzel, C.L., McCully, M.E., Canny, M.J., 1989. Development of water conducting

capacity in the root systems of young plants of corn and some other C4 grasses. Plant Physiol. 89, 1094–1101. http://dx.doi.org/10.1104/pp.89.4.1094.
Plant-environment interactions. In: Wilkinson, R.E. (Ed.), Books in Soils, Plants, and the Environment, 2nd ed. Marcel Dekker, New York.
Ye, Q., Steudle, E., 2006. Oxidative gating of water channels (aquaporins) in corn roots. Plant Cell Environ. 29, 459–470. http://dx.doi.org/10.1111/j.1365-3040.2005.01423.x.
Zarebanadkouki, M., Meunier, F., Couvreur, V., Cesar, J., Javaux, M., Carminati, A., 2016. Estimation of the hydraulic conductivities of lupine roots by inverse modelling of high-resolution measurements of root water uptake. Ann. Bot. 118 (4). http://dx.doi.org/10.1093/aob/mcw154. (mcw154).
Zimmermann, H.M., Hartmann, K., Schreiber, L., Steudle, E., 2000. Chemical composition of apoplastic transport barriers in relation to radial hydraulic conductivity of corn roots (Zea mays L.). Planta 210, 302–311. http://dx.doi.org/10.1007/PL00008138.
Zwieniecki, M.A., Thompson, M.V., Holbrook, N.M., 2002. Understanding the hydraulics of porous pipes: tradeoffs between water uptake and root length utilization. J. Plant Growth Regul. 21, 315–323. http://dx.doi.org/10.1007/s00344-003-0008-9.